Available online at www.sciencedirect.com

ScienceDirect

Procedia CIRP 125 (2024) 42–47

www.elsevier.com/locate/procedia

CIRP BioM 2024

FRESH 3D Bioprinting of Alginate – Cellulose – Gelatin Constructs for Soft Tissue Biofabrication

Miriam Seiti[a,b]*, Elena Laura Mazzoldi[c], Stefano Pandini[b], Silvia Giliani[c], Eleonora Ferraris[a], Paola Serena Ginestra[b], Elisabetta Ceretti[b]

[a]*Manufacturing Processes and Systems (MaPS), Mechanical Engineering, Campus De Nayer, KU Leuven, Belgium*
[b]*Department of Mechanical and Industrial Engineering, University of Brescia, Brescia, Italy*
[c]*Department of Molecular and Translational Medicine, "Angelo Nocivelli" Institute for Molecular Medicine, University of Brescia, ASST Spedali Civili, Brescia, Italy*

* Corresponding author Miriam Seiti. *E-mail address:* miriam.seiti@kuleuven.be

Abstract

The fabrication of three-dimensional (3D) bioprinted free-standing, low viscous, cell-laden hydrogels with good resolution, low cytotoxicity, and mechanical properties, comparable to native soft tissues, is a current challenge in tissue engineering. Recently, a new syringe extrusion approach, called Freeform Reversible Embedding of Suspended Hydrogels (FRESH), has been introduced to enhance 3D-bioprinting of soft hydrogels. Printing is conducted with the material embedded in a thermo-reversible gelatin bath, which acts as supporting material and can also initiate *in-situ* crosslinking when proper crosslinker agents are added. This work is the first to develop a 3D FRESH printable, low-cost, polymeric hydrogel composed of sodium alginate (SA), carboxymethylcellulose (CMC), and gelatin. A factorial design is investigated to identify best printing parameters. Printability *Pr* and *CAD fidelity* indexes are defined as responses of interest against scaffold resolution and shape fidelity. Results show a free-standing scaffold with a printability index, $Pr \sim 1$, a compression Young's Modulus of about 4 kPa, and a cellular ATP content of stromal cells up to 50% compared to a 2D cell culture after 14 days. These promising results demonstrate the potential of such hydrogel to print soft constructs, applicable for neural or skin tissue engineering applications.

Keywords: bioprinting; 3D FRESH printing; soft hydrogels; process optimization

Introduction

Bioprinting is a fast-growing additive manufacturing (AM) technology with unique applications in the biomedical field, including tissue engineering (TE) and 3D cell culturing. Bioprinting allows the deposition of bioinks in complex geometries following a computer aided design (CAD) pattern. Specifically, bioinks are hydrogels enclosing living cells, with specific fine-tuned compositions. Such hydrogels should have particular mechanical, biomechanical and biomimetic properties to mimic the *in vivo* cellular microenvironment, defined as extra cellular matrix (ECM). The ultimate goal of these bioinks is to use them for *in vitro* tissue models, both healthy and diseased, closer to the complex and intricate *in vivo* 3D ECM than traditional 2D culture models.[1]

During the last decade, bioprinting has been applied for the biofabrication of TE constructs using different techniques, including syringe-extrusion, inkjet and laser-assisted bioprinting.[2] However, this technology has not already reached clinical applications for limited knowledge on biocompatibility, cell behavior, precision, and reproducibility. [3] Ready-to-use cartridges are often very expensive and allow

10.1016/j.procir.2024.08.008

limited tuning of composition, rheological features, and polymerization mechanisms. The classical bioink formulations may include alginate, gelatin, collagen, fibrin, hyaluronic acid, and chitosan.[3] In addition, laminins and Matrigel® are both routinely used for the coating of cell culture vessels for 2D culture of particular cell types, but have been also extensively used as biocompatible compounds in bioinks. [4], [5] Syringe-extrusion bioprinting is the most used technique, in which a syringe, placed in the printing head, contains a bioink that is extruded through a nozzle on a vessel, placed on the printing plate. Temperature of printing head (T_h [°C]) and plate (T [°C]), nozzle diameter ($Ø$ [µm]), printing speed (s [mm/s]) and pressure (p [bar]), and also z-offset (z [mm]), are the main parameters which can be finely tuned to increase bioink printability, shape stability and fidelity. Nonetheless, resolution for syringe-extrusion bioprinting is limited in the range of 200-2000 µm and only viscous materials allow a layer-by-layer (LBL) deposition without sample collapse after printing.[6] However, highly viscous inks affect results reproducibility and cell viability, by increasing the shear stress through the nozzle.[7] Low viscous bioinks are then preferred, however they encounter limited shape fidelity due to printed filaments collapse after printing due to gravity force.

In this context, an emerging approach, referred as Freeform Reversible Embedding of Suspended Hydrogels (FRESH) method, is becoming the most ideal method to print soft and defined patterns. The FRESH method consists of a reversible bath in which the bioink is extruded and physically supported to maintain the desired 3D pattern.[8] To achieve this, the bath includes a minimal concentration of chemical crosslinking agents, which initiate an *in situ* crosslinking process. The sacrificial material is composed of a slurry, usually gelatin-based. In this case, gelatin is easily removed after bioprinting by melting at 37°C. Although numerous case studies have explored its application, a significant scientific gap remains, particularly concerning its use towards the biofabrication of soft constructs with precise shape fidelity.

The aim of this work is to exploit the FRESH method for the bioprinting of a low-cost, non-toxic, low-viscous cell-laden hydrogel towards the bioprinting of soft tissue constructs. Printing parameters are optimized by means of a design of experiment (DOE) approach. To the best of author's knowledge, this is the first time that a DOE approach is used to study bioink printability by applying the FRESH printing method. The bioink chosen is composed of sodium alginate (SA), carboxymethylcellulose (CMC), and gelatin, with embedded stromal cells for preliminary tests. SA is selected due to its low cost, good printability and biocompatibility, often employed to enhance the mechanical, and rheological properties of composite bioinks.[9] CMC is an unique micro-fibrillar FDA approved cellulose derivate chosen as thickener and which can act as fibrous ECM mimicker.[10] Lastly, gelatin provides cell binding sites and, after liquefaction at 37 °C, it increases the construct porosity and enhance cell infiltration. Laminin-521 and Matrigel® are also added in the formulation to increase cellular adhesion and proliferation. Ultimately, this manuscript provides additional insights into sterilizing bioink and FRESH bath. Various sterilization methods, including autoclaving, ultraviolet (UV) irradiation, filtration, exposure to ethylene oxide, and ethanol disinfection, can be employed.[11] In the present study, UV-irradiation, along with ethanol disinfection for bath preparation, is implemented.

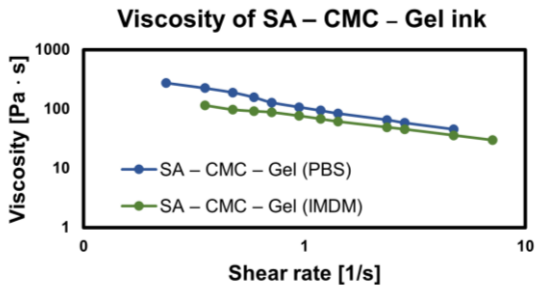

Figure 1. Viscosity of the SA–CMC–Gel bioink in 1x PBS and IMDM. Data partially obtained from Sughi et al. [13]

1. Materials & Methods

2.1 Bioink preparation

The SA–CMC–Gel bioink was prepared with 1.5 w/v% alginate low viscosity (SA, Thermo Fisher Scientific, Waltham, MA), 2.5 w/v% sodium carboxymethylcellulose (NaCMC, Mw = 250 kDa, Thermo Fisher Scientific), and 1 w/v% type A gelatin from porcine skin (Gel, Sigma Aldrich, Saint Louis, MO). The viscosity, η, of the bioink in 1x phosphate buffer solution (PBS, Euroclone) and IMDM is shown in **Figure 1**, as previously reported by the same research group. [13] In both mediums, the ink exhibits a gel-like shear-thinning behavior, making it suited for a bioprinting process. Weighed powders were UV-sterilized and then dissolved in sterile PBS or IMDM (bioprinting) in autoclaved glassware on a warm stirrer for 2 h. When indicated, Laminin-521 (Thermo Fisher Scientific) and Matrigel® Growth Factor Reduced (Corning, Corning, NY) were added at 1 µg/mL and 50 µg/mL of protein, respectively. The crosslinker $CaCl_2$ (Sigma Aldrich) was dissolved in Milli-Q water at 3 w/v% and autoclaved.

2.2 Gelatin Bath Preparation

Gelatin type A from porcine skin (Sigma Aldrich) was dissolved at a final concentration of 4.5 w/v% in $CaCl_2$ at a concentration of 10 mM. After gelification overnight at 4°C, gelatin underwent freezing at -20°C for 45 min, followed by blending and centrifugation in falcons of 50 mL at 3500 rpm for 2 min (repeated three times, with $CaCl_2$ refilling) to eliminate foam. Gelatin powder was UV-sterilized for 2 h and filled 6-well plates were further UV-sterilized for 2 h in ice.

2.3 Process investigation and methodology

Printing experiments were carried out using the 3D-Bioplotter system (EnvisionTEC, DE), equipped with the low-temperature print head (**Figure 2A**). After maintaining the bioink at 10°C for 1 h in the print head, constructs were printed in the FRESH bath and further crosslinked with $CaCl_2$ for 20 min at 37°C, as shown in **Figures 2B-C**. Afterwards, the samples were washed with twice with DMEM (Euroclone

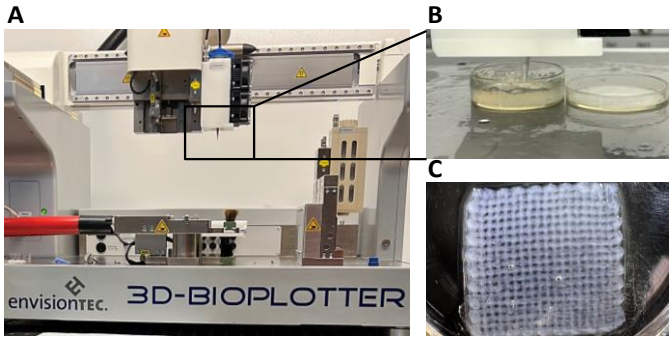

Figure 2. Representative images of A) the 3D-Bioplotter (EnvisionTec) using B) the FRESH approach with the gelatin bath, and C) the final printed scaffold.

Table 1. Experimental campaigns for 3D FRESH (bio)printing.

1. Experimental campaign 3D FRESH (bio-)printing (22°C, 55% rh)				
Parameters	**Values**			
Print speed *s* [mm/sec]	5	10	15	20
Control pressure *p* [bar]	1.5		2	
Response	Printability index, *Pr* [#], CAD fidelity [#]			
Fixed Parameters	**Values**			
Substrate	Petri dish, Ø 45 mm or 6-well plate			
Needle diameter	21G			
Stand-off distance *z* [mm]	0.5			
Number of layers *n* [#]	11			
Platen temperature T_p [°C]	5			
Print head temperature T_h [°C]	10			
FRESH bath formulation	4.5 w/w% Gel – 10 mM $CaCl_2$			
Post-printing crosslinking $CaCl_2$	3 w/w% for 20 min			
Sample	Cross-hatched mesh 20x20 mm, pore 1 x 1 mm			

Milan, Italy) and kept in the incubator (5% CO_2). A factorial DOE was conducted considering the print speed s = (5, 10, 15, 20) mm/s and the print pressure p = (1.5, 2) bar, with three replicas each. The details of the experimental study are reported in **Table 1**. As response of interest, a Printability Index (*Pr*) was calculated as in Ouyang et al., according to the following equation [14]:

$$Pr = \frac{\pi}{4}\frac{1}{C} = \frac{L^2}{16A}, \text{ with } C = \frac{4\pi A}{L^2} \qquad (Eq.1)$$

Here, A [mm^2] represents the pore area, and L [mm] stands for the pore perimeter. Under ideal hydrogel gelation and printing conditions, each pore within the printed mesh aligns precisely with the CAD design, forming a 1 x 1 mm square. Consequently, $C = \pi/4$ and $Pr = 1$. As second response of interest, a CAD fidelity index [#] was determined by computing the ratio between A and the perimeter, P [mm], to the ideal CAD values of A = 1 mm^2 and P = 4 mm, respectively.

2.4 Samples characterization

2.4.1 Optical characterization

Microscopic images were captured using the Hirox KH8700 (JP) microscope. For every mesh, the software ImageJ was employed to analyze the central region, measuring an area of 1 x 1 cm. This process was conducted for a total of 15 pores per mesh, resulting in 45 data points for each condition, using the "Analyze Particles" function. Data were computed for each printing condition.

2.4.2 Compression test

Compression test was conducted on cylindrical meshed samples of 3D FRESH printed SA and SA-CMC-Gel hydrogels. These samples had a diameter of about $Ø$ = 4.5 mm and a height of about h = 3.5 mm. The experiments were carried out at 25°C using a Dynamic-Mechanical Analyzer (DMA Q800 - TA Instruments) equipped with a load cell with a maximum capacity of 18 N. Each test had three replicas.

2.4.3 Cellular biocompatibility

MS5 cells were provided by Dr. Anna Villa, San Raffaele Telethon Institute for Gene Therapy, Milan, Italy. MS5 cells were cultured in DMEM medium supplemented with 10% fetal bovine serum (FBS), 1% penicillin/streptomycin, and 1% L-glutamine (all purchased from Euroclone), at 37 °C, 5% CO_2 in a humidified incubator. Cells were detached using trypsin-EDTA (Euroclone) when confluent. Cells were expanded, detached, counted, and centrifuged. The cell pellet was gently resuspended in the bioink by using a sterile syringe without needle, to obtain a homogeneous concentration of 1 x 10^6 cells/mL. The cell-loaded bioink was extruded using a syringe (i.e. not printed sample) or moved into a sterile cartridge Optimum Class VI, 30 cc (Nordson, Westlake, OH) for the bioprinting process (i.e. printed sample). As a control, an equal amount of cells were 2D cultured on plastic vessels.

Preliminary biocompatibility tests were firstly performed on the bioink and gelatin bath to verify their non-toxicity, secondly on the bioink supplemented with Laminin-521 and Matrigel®, and finally after the bioprinting process. For the first experiment, the bioink (~ 500 µL) was poured by solely utilizing a syringe into a well containing the support bath, without undergoing bioprinting. In parallel, the same amount of bioink was dispensed in a well of a 24-well plate without gelatin bath. The bath-containing multi-well plates were further exposed to UV light for an additional 1 h on ice after being filled. In the second test, Laminin-521 and Matrigel® were added in the SA-CMC-Gel bioink composition respectively. The final ink was evaluated without the use of the support bath, in order to eliminate any potential additional factors in the bioink analysis. The third study was conducted to assess the viability of bioprinted MS5 using the 3D FRESH method. The best parameter conditions obtained from the printability analysis were used to print the bioink. As comparison, samples fabricated using a solely syringe and 2D cell culture controls were parallely examined with printed samples. Sterilization was performed as detailed in the second experiment.

Cell viability was assessed by both Live/Dead staining and ATP cell viability assay. For Live/Dead staining, the LIVE/DEAD™ cell imaging kit (488/570, Thermo Fisher Scientific) was employed. After 24 h of culture, a slice of cell-loaded hydrogels was incubated at room temperature (RT) for 15 min in the dark with Live/Dead 1X in complete DMEM. The hydrogel was put between two microscope slides and fluorescent images from at least 5 fields were acquired at Olympus IX70 fluorescence microscope (Olympus, Tokyo, Cybernetics, Rockville, MD). For the ATP cell viability assay, the CellTiter Glo® 3D cell viability assay (Promega, Madison,

WI) was employed, which produces a chemiluminescent reaction due to ATP-dependent luciferin oxidation. Cell-loaded hydrogels were incubated at RT in the dark for 20 min with the kit substrate in a 1:1 ratio to induce cell lysis and ATP release. The mix was then moved to a black 96-well plate, 150 µL/well, in technical replicates (at least three). After 10 min, the signal was acquired with an Infinite M200 microplate reader (Tecan, Männedorf, Switzerland). The ATP concentration was calculated from the mean of replicates using an ATP standard curve. Data were expressed as percentage of 2D culture at t0. The analyzed time points were: t0, 24 h, 48 h, 7 days, and 14 days, as indicated.

Micrographs were obtained from EVOS™ XL Core Imaging System (Thermo Fisher Scientific, IT).

3. Results & Discussion

3.1 Printability and process analysis

Figure 3 displays optical images of the SA–CMC–Gel ink 3D FRESH printed under various conditions as part of a DOE factorial design. In particular, the centered printed grids are reported for each condition, along with representative images of all constructs printed at p = 2 bar. The inks demonstrated printability under all conditions, except for the one with s = 5 mm/s and p = 2 bar. Noticeable variations in pore and shape definition are depicted across different conditions.

The definition and geometry of the printed pores are usually better when the pressure is set to p = 2 bar. Under a pressure of p = 1.5 bar, the pores exhibit irregular shapes, and the printed strands display unevenness with bumps along their surface. Layers of the printed mesh also lack proper alignment. Conversely, at a pressure of p = 2 bar, there is a noticeable printability enhancement, including more open pores (except

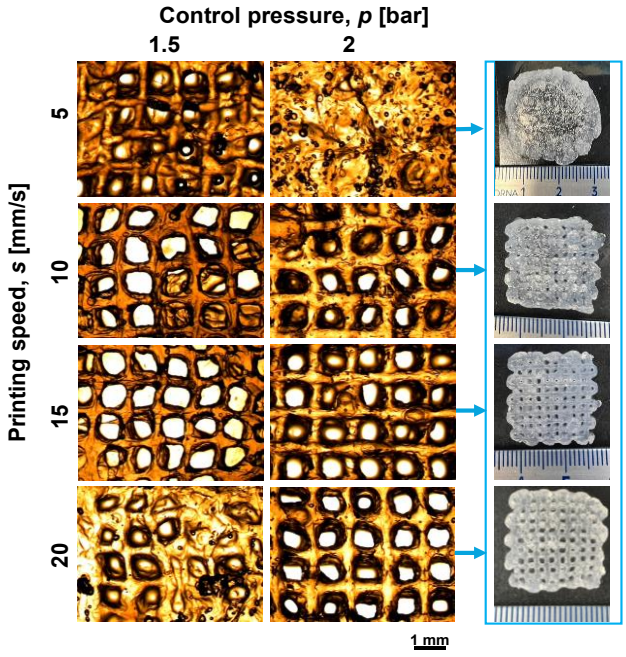

Figure 3. Representative optical images of 3D FRESH printed SA–CMC–Gel hydrogels under the DOE factorial print conditions analyzed.

for the condition p = 2 bar and s = 5 mm/s), a well-defined grid pattern, and pores that closely resemble circular or rectangular shapes rather than being entirely irregular.

The *Pr* indexes presented in **Figure 4A** support these visual observations, showing a *Pr* value *Pr* = 1.03 ± 1e-2 for the condition p = 1.5 bar at s =10 mm/s, a *Pr* = 1.07 ± 1e-2 at p = 1.5 bar and s =15 mm/s, and a *Pr* =1.16 ± 0.1 at p = 2 bar and s =20 mm/s. The CAD fidelity index employed as second response of interest also validated these results. As depicted in **Figure 4B**, the condition with a CAD fidelity index for both area (A = 0.74 ± 1e-2 mm^2) and perimeter (P = 0.86 ± 1e-2 mm) nearly equal to 1 (representing the ideal condition) corresponds to p = 1.5 bar and s = 10 mm/s. The second best condition is at p = 2 bar and s = 20 mm/s, having an A = 0.57 ± 1e-2 mm^2 and a P = 0.80 ± 1e-2 mm. In conclusion, the conditions p = 1.5 bar at s =10 mm/s and p = 2 bar at s =20 mm/s result as the most suitable print conditions. However, as also evident from **Figure 3**, the second condition is preferred since the strand filament is more uniform. This result underscores the need to consider the strand uniformity as response of interest in future studies.

3.2 Mechanical properties

Figure 4C depicts the stress *vs.* strain curves measured under compression on 3D FRESH printed SA and SA-CMC-Gel scaffolds. Both scaffolds exhibit a mechanical response that may be considered akin to that of an expanded, or cellular, elastomer: three regions are highlighted: i) an initial quasi-elastic region within the first 10% strain, followed by ii) a region with lower slope extending to approximately 50% strain, and finally iii) by a sudden stiffness increase when entering the densification region. A compressive Young's Modulus was therefore tentatively evaluated as slope of the curve in the first region: for the SA hydrogel its value is E(50%) = 30.0 ± 1.4 kPa, whereas for the SA-CMC-Gel hydrogel, it is E(50%) = 4.4 ± 0.4 kPa. This indicates that the incorporation of CMC and gelatin in the ink composition of SA-CMC-Gel contributes to a reduction in the Young's Modulus, a quality desirable for soft tissues, such as the nervous one, which typically exhibit a Young's Modulus lower than 10 kPa.[15]

3.3 Cellular biocompatibility

3.3.1 Gelatin bath and bioink

At first, the influence of the bioink and the gelatin bath on cellular viability was assessed. **Figures 5A-B** reports the micrographs of 3D cellular attachment with and without gelatin. ATP test at t0 reveals that both hydrogels in or not in bath present a cell metabolic activity of about 50% of cells in 2D culture, with the no-bath sample showing a slightly higher one. However, the metabolic activity dramatically increases in both conditions after 24 h, reaching the same levels of 2D culture, without remarkable differences between bath and no-bath samples (see **Figure 5A**). Live/Dead staining at 24 h also confirms that almost all cells in both bath and no-bath samples are alive, as demonstrated by the predominance of green spots. Nevertheless, as shown in **Figures 6** and **5**, cells exhibit a round shape compared to the 2D control (**Figure 5E**) indicating that

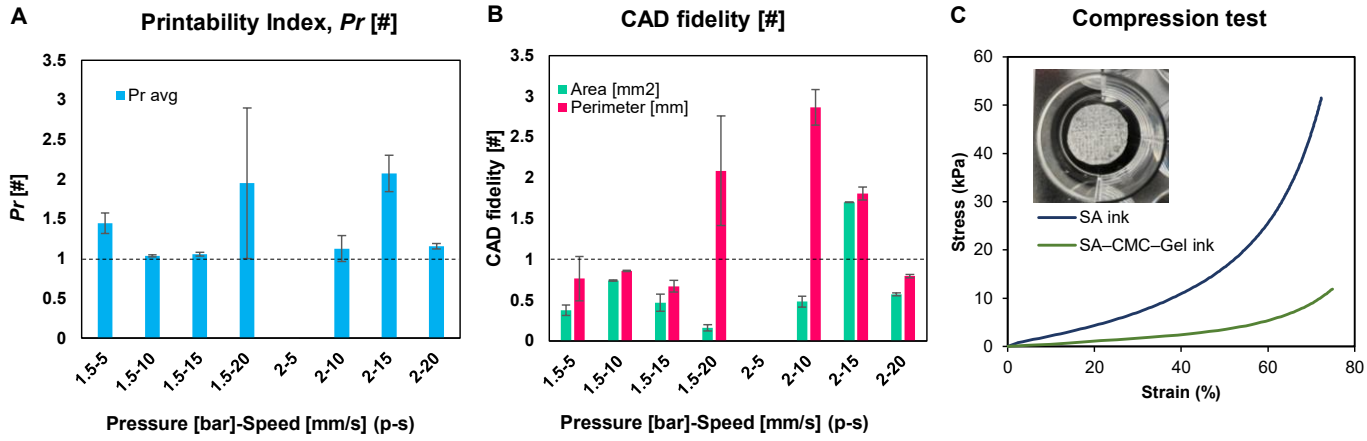

Figure 4. Results and characterization on the 3D FRESH printing samples: A) printability index *Pr* [#] and B) *CAD fidelity* index, [#] expressed as A [mm^2] and P [mm] for each print condition using the SA–CMC–Gel hydrogel; C) compression test (stress *vs.* strain plot) of 3D FRESH printed SA and SA–CMC–Gel hydrogels.

they are unable to spread freely within the material. Still, the bioink can sustain cellular viability and the presence of gelatin bath does not impact on cell viability. However, the experiment could not be extended to longer time points due to bacterial contamination, which was widespread in bath samples and randomly in no-bath samples. This indicates that relying only on a UV irradiation period of 1 h, widely reported in the literature, is not sufficient to sterilize the gelatin bath. The main cause is mostly related to the use of a blender in its preparation, which cannot be autoclaved. Consequently, other sterilization methods, such as autoclaving or gamma ray irradiation, are strongly recommended for future studies. [12]

3.3.2 Bioink enhancement with ECM-derived proteins

To increase cell spreading and promote proliferation, Laminin-521 and Matrigel® were incorporated in the SA-CMC-Gel ink. Micrographs at 24 h shows an increased cellular population in the presence of Laminin/Matrigel (L/M) (**Figures 5C-D**). However, ATP test at t0 reveals a comparable metabolic activity between samples with L/M and samples without Laminin/Matrigel (no L/M), which is around 70% of cellular viability in 2D culture, as shown in **Figure 6C**. ATP content stays constant until day 7, with a reduction in L/M enriched samples. Notably, the ATP levels in 2D cell cultures are assessed up to 48 h, as cells quickly reached over confluence and got detached. Live/Dead staining at 24 h further verifies that nearly all cells in both conditions exhibit a green fluorescence, indicating viability. However, they still maintain a round shape, suggesting that the incorporation of Laminin and Matrigel®, at the selected concentrations, does not provide any advantage in terms of cell spreading.

Future tests will assess the effect of increasing Laminin and Matrigel® concentrations.

3.3.3 Bioprinting process

Figure 5F shows 3D cellular growth and attachement in FRESH bioprinted constructs. As depicted in **Figure 6E**, ATP test at t0 reveals a comparable metabolic activity between printed and not printed samples, between 20-30% of cells' viability of 2D control. The ATP content is further tripled at 24 h in the not printed samples, but increases to a lower extent in

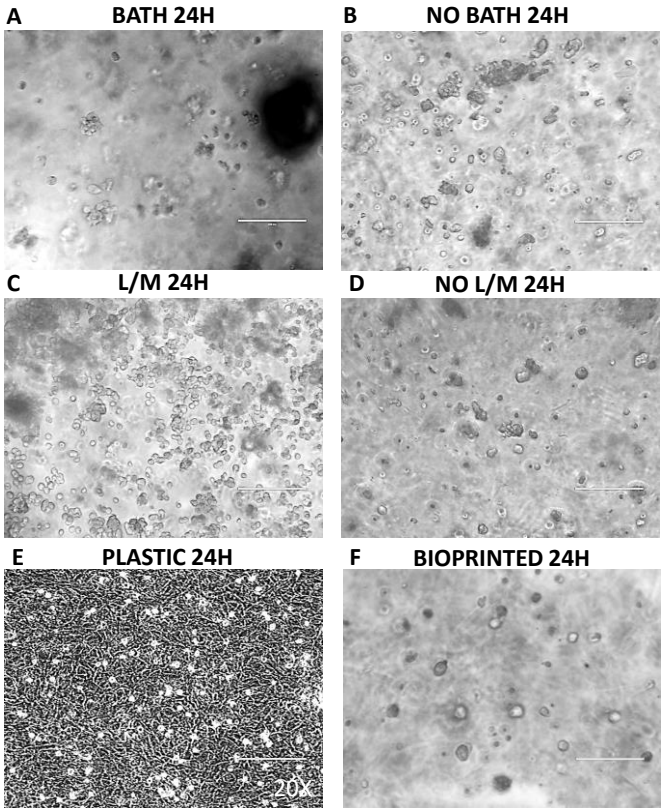

Figure 5. Micrographs *of MS5 cells in samples at 24 h:* A,B) with and without gelatin bath, C,D) not printed construct with and without Laminin-521 and Matrigel®, E,F) 2D control sample and bioprinted construct. Scale bar: 200 µm.

the printed ones. In both cases, ATP content remains constant over the time, with no further increase. Live/Dead staining at 24 h confirms that the majority of cells in both conditions are alive, but still round-shaped. Live/Dead staining after 7 days also reveals no remarkable differences (data not shown). Moreover, in these tests, the UV-sterilization time was extended up to 2 h, and it showed to be effective but not entirely sufficient. Over the course of a week, a few random wells indeed exhibited bacterial contamination, particularly in the printed plates.

ATP content of bioprinted samples at day 14 is comparable to previous timepoints (**Figure 5E**). However, not printed samples got disintegrated while discarding the culture

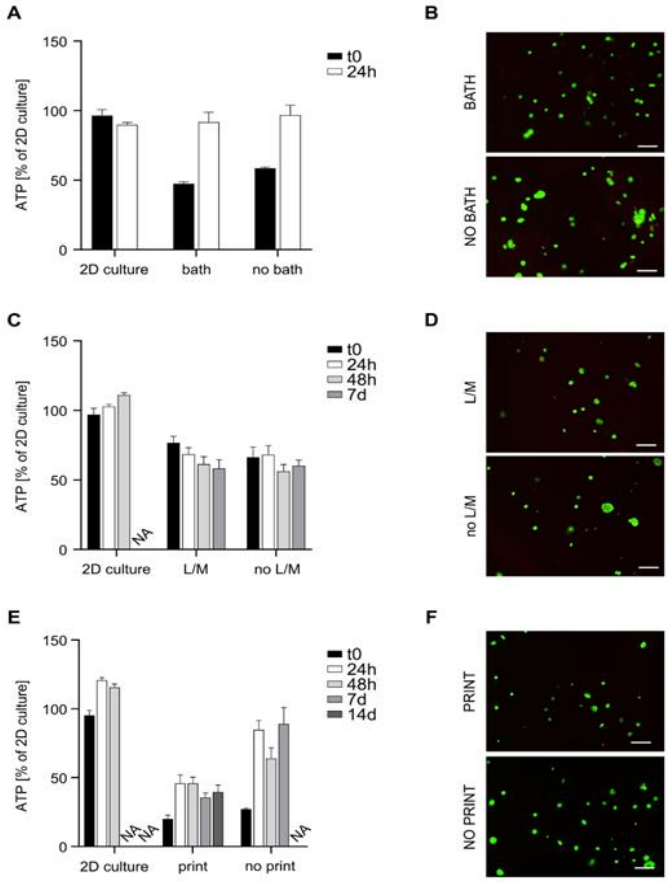

Figure 6. *Biocompatibility assays evaluation.* ATP content SA–CMC–Gel bioinks as percentage of t0 2D cell culture and representative Live/Dead staining images at 24 h. Green=live cells; Red=dead cells. Scale bar: 100 µm. Data shown as (µ±σ) of at least three technical replicates. NA = not available. A,B) ATP of not printed bioinks with or without gelatin bath at t0 and t24h and relative Live/Dead assay. C,D) ATP of not printed bioinks with or without Laminin-521 and Matrigel® at t0, 24h, 48h and 7 days and Live/Dead assay. E,F) ATP of 3D FRESH bioprinted and not printed bioinks at t0, 24h, 48h, 7 days and 14 days and Live/Dead assay.

supernatant due to their fragility. Instead, because of the improved crosslinking made possible by the grid-shaped geometry, the bioprinted constructs increased their stability.

4. Conclusions and future perspectives

Developing bioinks capable of being bioprinted in intricate geometries is a current challenge in the advancement of 3D cell culture models. Ongoing research is focusing on the development of low-viscosity bioinks capable of maintaining good printability and shape fidelity towards soft tissues biofabrication. 3D FRESH bioprinting is an emerging syringe extrusion-based approach which facilitates the bioprinting of such hydrogels into complex 3D shapes.

This manuscript deals with the bioprinting of a low-cost, nontoxic, own-developed SA-CMC-Gel bioink. A factorial DOE was undertaken to identify the best printing parameters, utilizing two responses of interest, that is a *Pr* and *CAD fidelity* index, for scaffold resolution and shape fidelity. 3D FRESH free-standing samples were printed at $p = 2$ bar and $s = 20$ mm/s with a *Pr* value of 1.16 ± 0.1 and a *CAD fidelity* index with $A = 0.57 \pm 1e\text{-}2$ mm² and $P = 0.80 \pm 1e\text{-}2$ mm. Final scaffolds showed a compression Young's Modulus of E(50%) = 4.41 ± 0.4 kPa, aligning well with the stiffness of the nervous tissue, having a E between 3.5 and 10 kPa.[14]

Stromal cells (MS5) were chosen for biocompatibility tests. Both the bioink and the gelatin bath were biocompatible, with the latter not influencing the biocompatibility of the former. The addition of Laminin-521 and Matrigel® in the bioink, aimed at improving cellular protrusions, was not sufficient to prevent a round shape of cells, likely due to the low concentrations selected. Final 3D FRESH bioprinted constructs exhibited a cellular ATP content at day 14 up to 50% compared to a 2D cell culture, maintaining their shape up to 14 days, in contrast to no-printed constructs which lasted till day 7. UV exposure alone revealed to be insufficient to achieve complete sterilization of the gelatin bath and bioink. Autoclaving is then recommended to reduce bacterial contamination. This process is known to generate a denaturation of natural based proteins, such as gelatin, albeit retaining its cellular binding sites. Future tests will explore this option, along with bioink and bioprinting optimization.

Acknowledgements

The authors acknowledge Research Foundation Flanders (FWO) for the doctoral fellowship of Miriam Seiti, 1SB1120N, Alessandro Nocivelli for Elena Laura Mazzoldi's fellowship, and Alessandro Nocivelli and Angelo Nocivelli Foundation for project fundings.

References

[1] J.H.Park, et. al. 3D Printing of Tissue/Organ Analogues Containing Living Cells, Ann. Biomed. Eng. 2017; 45(1):180–194.
[2] P.Bartolo, et. al., 3D bioprinting: Materials, processes, and applications, CIRP Ann. 2022;71(2):577–597.
[3] S.Tripathi, et. al., 3D bioprinting and its innovative approach for biomedical applications, MedComm 2023;4(1):e194.
[4] R.M.Ferraro, et. al., Establishment of 3 iPSC lines from fibroblasts of a patient with Aicardi Goutieres syndrome mutated in RNaseH2B., Stem Cell Res. 2019, 41,101620.
[5] M.Jury, et. al., Bioorthogonally Cross-Linked Hyaluronan–Laminin Hydrogels for 3D Neuronal Cell Culture and Biofabrication, Adv. Healthc. Mater. 2022;11(11):2102097.
[6] S.Tian, et. al., Key parameters and applications of extrusion-based bioprinting, Bioprinting 2021,23, e00156.
[7] J.Karvinen, M.Kellomäki, Design aspects and characterization of hydrogel-based bioinks for bioprinting, Bioprinting 2023, 32:e00274.
[8] T.J.Hinton, et. al.,3Dprinting of complex biological structures by freeform reversible embedding of suspended hydrogels, Sci. Adv. 2015;1(9): e1500758.
[9] Y.J.Choi, et. al., 3D Bioprinting of In Vitro Models Using Hydrogel Bioinks, Polymers 2021, 13(3):366.
[10] A.Zennifer, et. al., Key advances of carboxymethylcellulose in tissue engineering & 3D bioprinting applications, Carbohydr. Polym. 2021,256:117561.
[11] T.Lorson, et. al., Sterilization Methods and Their Influence on Physicochemical Properties and Bioprinting of Alginate as a Bioink Component, ACS Omega 2020, 5(12):6481–6486.
[13] S.Sughi, et. al., Assessing the Viscosity of Alginate-Cellulose-Based Hydrogels, Lect. Notes Networks Syst. 2023;745:510–522.
[14] L.Ouyang et al., Effect of bioink properties on printability and cell viability for 3D bioplotting of embryonic stem cells, Biofabrication 2016;8:035020.
[15] H.Zhao, et. al., Research Progress on the Flexibility of an Implantable Neural Microelectrode, Micromachines 2022;13(3):386.